Available online at www.sciencedirect.com
ScienceDirect
Journal of Catalysis 249 (2007) 234–243
JOURNAL OF CATALYSIS
www.elsevier.com/locate/jcat

A FT-IR study of deactivation phenomena during methylcyclohexane transformation on H-USY zeolites: Nitrogen poisoning, coke formation, and acidity–activity correlations

G. Caeiro [a,b], J.M. Lopes [a], P. Magnoux [b], P. Ayrault [b], F. Ramôa Ribeiro [a,*]

[a] *IBB—Institute for Biotechnology and Bioengineering, Centre for Biological and Chemical Engineering, Instituto Superior Técnico, Av. Rovisco Pais, 1049-001 Lisboa, Portugal*

[b] *Laboratoire de Catalyse en Chimie Organique, Chimie 7A-3, 40 Avenue du Recteur Pineau, 86022 Poitiers Cedex, France*

Received 9 November 2006; revised 30 March 2007; accepted 9 April 2007

Available online 8 June 2007

Abstract

The present work discloses some of the less clear aspects regarding the deactivation of acidic USY zeolites due to coke formation and poisoning with basic nitrogen molecules (3-methylpyridine, 2,6-dimethylpyridine, and quinoline). Coke formation occurs essentially in the supercages; consequently, the Brønsted acid sites located in these structures lose their activity quite rapidly. Nitrogen-containing molecules also interact preferentially with the Brønsted acid sites located in the supercages. 2,6-Dimethylpyridine has a higher poisoning ability than the other two bases, probably due to steric hindrance, which limits the interaction with the nonactive Lewis sites. (Only Brønsted acid sites are poisoned, and hence deactivation is more pronounced.) This work also demonstrates that quantification of the PyH^+ band on pyridine adsorption is an inaccurate method for determining the decrease in the number of Brønsted acid sites during the deactivation of catalytic cracking catalysts. Indeed, only the surface of the hydroxyl vibration bands can be used to determine the decrease in the number of accessible active sites. Acidity–activity correlations show that only the Brønsted acid sites located in the supercages are active in methylcyclohexane transformation; as a result, an average turnover frequency for these sites can be determined with the slope of the activity versus acidity curve (0.33 s^{-1}).

Keywords: IR spectroscopy; H-USY zeolite; Catalytic cracking; Coke formation; Nitrogen poisoning; Acidity–activity correlations

1. Introduction

Fluid catalytic cracking (FCC) is one of the key processes in a modern refinery [1], producing very important amounts of gasoline and light olefins. Currently, the main active component in FCC catalyst is the H-USY zeolite; it can be obtained by hydrothermal treatment (steaming) of the Y zeolite structure [2–5]. Rare-earth cations are commonly added to H-USY to reinforce its structure and prevent dealumination at high temperatures in the presence of steam [6–8].

Acid zeolites, like H-USY, are strongly deactivated during cracking reactions, mainly due to the formation of polyaromatic compounds known as coke [9,10]. Along with hydrocarbons, feedstocks also contain nonnegligible amounts of metals, nitrogen, and sulfur compounds, which also can have a deactivating effect. The FCC feed constitutes mainly vacuum gas oil, which contains approximately 25–30% of the nitrogen existing in crude oil [11]. Nevertheless, over the last few years, increasing amounts of vacuum residue have been added to FCC feedstocks, increasing the nitrogen content of the charge. The presence of these poisons is critical; due to the decrease in acid sites resulting from the regeneration step, FCC catalysts are particularly sensitive to the presence of basic poisons in the feed [12–15].

After nearly 50 years of intensive application, Fourier transform infrared (FT-IR) remains the most widely used, and usually most effective, spectroscopic method for characterizing the surface chemistry of heterogeneous catalysts [16]. Hydroxyl groups (possible Brønsted acid sites) may be detected and char-

* Corresponding author. Fax: +351 21 841 9018.
E-mail address: ramoa.ribeiro@ist.utl.pt (F. Ramôa Ribeiro).

0021-9517/$ – see front matter
doi:10.1016/j.jcat.2007.04.005

Table 1
Chemical composition and structural properties of the studied H-USY zeolite

Unit cell formula[a]	Si/Al[a]	$(Si/Al)_{fr}$[b]	Crystallite[c] (μm)	V_{micro} ($cm^3\,g^{-1}$)	S_{ext} ($m^2\,g^{-1}$)
$Na_{0.6}H_{29.4}Al_{30}Si_{162}O_{384}$, 26EFAl	2.8	∼5.4	∼0.5	0.293	28

EFAL: extra framework aluminum species
[a] Global Si/Al determined by ICP-AES coupling (inductively coupled plasma–atomic emission spectrometry).
[b] Framework Si/Al determined by X-ray diffraction.
[c] Measured by SEM (scanning electron microscopy).

acterized by IR spectroscopy through two distinct methodologies: (i) studying their vibration modes (OH fundamental, overtone, and combination vibrations) and (ii) studying their interaction with appropriated probe molecules. Ammonia, pyridine, or less basic molecules are usually used in the characterization of zeolite Brønsted acid sites.

Pyridine, the probe used in this work, produces a band at around 1545 cm^{-1} when adsorbed on Brønsted acid sites (PyH^+); the interaction results in formation of a pyridinium ion. Several extinction coefficients for the ∼1545 cm^{-1} band have been published [17–22]. Besides Brønsted acid sites, zeolites contain Lewis acid sites, which are not directly responsible for catalytic cracking but can play other roles. The coordination of pyridine with Lewis acid sites gives rise to a band at around 1454 cm^{-1} (PyL). The pyridine extinction coefficients used in this work were 1.13 $cm\,\mu mol^{-1}$ for the PyH^+ band and 1.28 $cm\,\mu mol^{-1}$ for the PyL band [22].

Throughout this study, IR spectroscopy was used to study some of the deactivation mechanisms, namely coke formation and poisoning with basic nitrogen molecules (3-methylpyridine, 2,6-dimethylpyridine, and quinoline) occurring over a protonic USY zeolite ($Si/Al_{fr} = 5.4$) during methylcyclohexane transformation. A temperature of 350 °C was selected, because a higher temperature would hinder comprehension of the two focused phenomena. The molecules retained in the zeolite were characterized both qualitatively and quantitatively. Moreover, the activity and Brønsted acidity were determined for several reaction times, and a correlation between the two measurements was obtained.

2. Experimental

The USY zeolite was supplied by PQ (reference CBV500). The protonic form was produced by calcination at 500 °C. Table 1 includes its chemical compositions and structural properties. In the catalytic tests, the reactor feed consisted of 10 mol% liquid methylcyclohexane reactant (Sigma–Aldrich, 99% pure) and 90 mol% N_2 (Air Liquide 99.9995% pure). In the poisoning tests, 540 ppm of basic nitrogen was introduced into the reactor feed. Three bases were selected: quinoline (Sigma–Aldrich, 99% pure), 2,6-dimethylpyridine (Sigma–Aldrich, 99% pure), and 3-methylpyridine (Sigma–Aldrich, 99% pure). The experimental tests were carried out in a Pyrex fixed-bed reactor; the reactions occurred in the gas phase at a pressure slightly above atmospheric (1.05×10^5 Pa). The liquid reagent was injected at a constant rate by a B-BRAUN SECURA perfusor. The rate of nitrogen was maintained constant with a BROOKS mass flow controller (5850 TR series).

The deactivation profiles were obtained by taking samples of the reactor effluent for different time on stream (TOS) values: 1, 15, 60, and 240 min. (Obtaining a constant methylcyclohexane partial pressure in the reactor inlet feed took 1 min.) This was achieved by using a 10-loop high temperature (200 °C) multiposition valve supplied by VICI. The reactor effluent sample analysis was carried out in a SHIMADZU GC-14B GC chromatograph with a Chrompack Plot Al_2O_3/KCl capillary column (50 m). Nitrogen was used as carrier gas with an inlet pressure of 1.5×10^5 Pa. A flame ionization detector with hydrogen flow of 40 $ml\,min^{-1}$ and an air flow of 500 $ml\,min^{-1}$ was used.

The FT-IR measurements were carried out in a Nicolet 750 MAGNA-IRTM spectrometer. An airtight system, in which the partial pressure of pyridine could be rigorously controlled, was needed. This closed system could be operated at two different vacuum levels: primary (1×10^{-2} Pa) and secondary (1×10^{-4} Pa). As before, the wafers (5–15 mg/cm^2) were initially pretreated at 200 °C for 1 h for the coked samples and at 400 °C overnight for the fresh samples. After the entire system was evacuated using the secondary vacuum system, the probe molecule was introduced into the system through a manual valve connecting the airtight system with the pyridine (Sigma–Aldrich, IR spectroscopic grade) container. The chemisorption was done for 15 min at 150 °C with a large excess of nitrogenated base. The physisorbed pyridine was removed for 1 h at the same temperature, after which the IR spectrum was collected. For fresh samples, a stepwise desorption (at 150, 250, 350, 450, and 500 °C) was carried out to evaluate the strength of the acid sites.

3. Results and discussion

3.1. Fresh zeolite characterization

Several distinct –OH groups can be identified in the IR spectra of acid zeolites. For the H-USY(5) zeolite, bands are observed at 3525, 3560, 3600, 3625, 3665, and 3735–3745 cm^{-1}. To distinguish between the bands of accessible Brønsted acid sites and those of nonacidic or inaccessible hydroxyls, pyridine was adsorbed on the catalysts; the bands corresponding to the acidic groups were identified by noting the difference between the spectrum of H-USY alone and that obtained after pyridine adsorption.

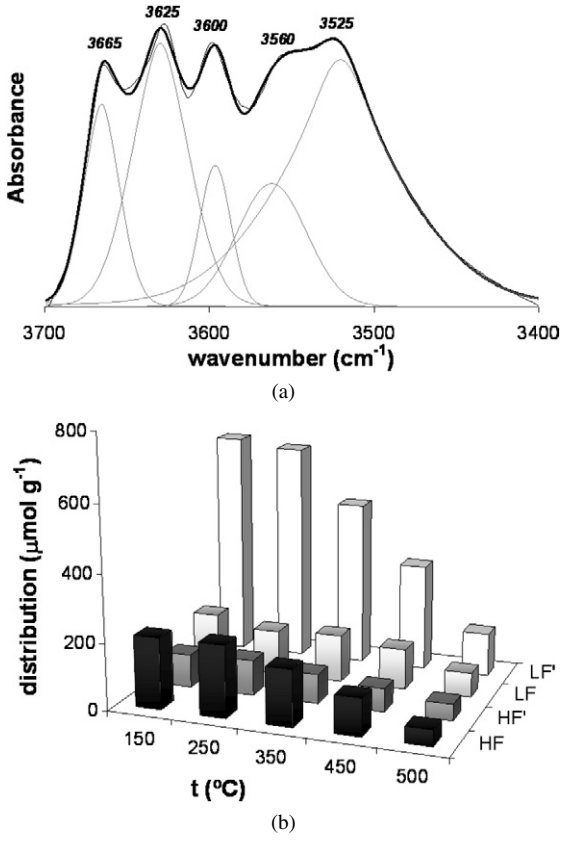

Fig. 1. (a) Deconvolution of the bands corresponding to the potentially active –OH groups (before adsorption minus after pyridine adsorption). (b) Brønsted acid sites density vs temperature: (black) HF, (dark gray) HF′, (light gray) LF, and (white) LF′.

The relative intensity of the bands corresponding to potentially active –OH groups (3700–3500 cm^{-1}) [17,21,23–25] can be determined by deconvolution (Fig. 1a). The bands at 3625 and 3560 cm^{-1} are the typical high-frequency (HF) and low-frequency (LF) –OH bands of the Y zeolite, corresponding to bridging hydroxyls in the supercages and in the sodalite cages, respectively. On the other hand, the bands at 3525 (LF′) and 3600 cm^{-1} (HF′) correspond to the same Al–OH–Si groups but after undergoing delocalization due to interaction with extra-framework species. The origin of the band at 3665 cm^{-1} also merits discussion. They present an acid strength between that of traditional Al–OH–Si groups and that of hydroxyl groups linked to extra-framework Al species. They have been proposed to correspond to partial framework (OH)Al–O–Si groups existing in defects produced during steaming treatment [27].

The extinction coefficients have been published previously [17,21]; consequently, the amount of each type of acid site (able to retain pyridine at 150 °C) also can be determined (Table 2). Comparing the global acidity measured experimentally (1146 μmol g^{-1}) with the theoretical one based on the amount of FAl species (2402 μmol g^{-1}) demonstrates that not all the Al–O–Si groups originate a Brønsted acid site able to retain pyridine at 150 °C.

Fig. 1b represents the amount of Brønsted acid sites able to keep the pyridine molecule adsorbed at several temperatures. This value can be considered a measurement of acid strength; however, correlations between this distribution and the catalyst activity were not yet proven reliable. The LF′ band seems to be the one more perturbed by temperature. Conversely, the amount of Brønsted acid sites characterized by the high-frequency bands, particularly the HF′ ones, does not decrease as rapidly on heating. These hydroxyl groups characterized by the HF′ –OH band are those able to retain pyridine at higher temperatures, and, consequently, they must be stronger. This heterogeneity of protonic sites can be explained by the presence of bridging hydroxyls with various numbers of Al atoms near the Al–OH–Si groups.

In terms of the Lewis acid sites, the following evolution of PyL species with temperature is observed: 150 °C (198 μmol g^{-1}), 250 °C (139 μmol g^{-1}), 350 °C (115 μmol g^{-1}), 450 °C (110 μmol g^{-1}), and 500 °C (26 μmol g^{-1}).

3.2. H-USY zeolite deactivation

Fig. 2a presents the deactivation due to coke and basic nitrogen for a contact time (inverse of the weight hourly space velocity) of 6 min during methylcyclohexane transformation over H-USY. A pronounced deactivation occurs in the first minutes of the reaction even for the tests with methylcyclohexane alone, due to coke formation. Basic nitrogen increase deactivation, with the difference more evident for long TOS. Moreover, the three bases do not cause the same deactivation for this contact time; the following order is seen: 2,6-dimethylpyridine > quinoline > 3-methylpyridine.

Fig. 2b represents the experimental nitrogen content (i.e., the actual amount in the zeolite) versus the amount calculated on the basis of the injected amount of nitrogen base. Three distinct regions can be identified: (1) All injected quinoline is retained in the zeolite (<0.4–0.5 wt% N); (2) the zeolite continues to adsorb quinoline, but only a fraction of the amount present in the feed (<1.0 wt% N); and (3) the H-USY zeolite becomes saturated and stops adsorbing the nitrogen base. This amount corresponds to ∼780 μmol g^{-1}, which corresponds to 70% of the Brønsted acidity calculated with the Al–OH–Si group IR bands and only 60% of the global acidity (Lewis + Brønsted).

There seems to be no difference between the adsorbed amounts of each base; consequently, the observed differences in the poisoning ability of the bases are not due to differences in the number of molecules retained in the zeolite. It seems that 2,6-dimethylpyridine is a stronger poison than the other two basic molecules; the same nitrogen content produces greater de-

Table 2
Amount (μmol g^{-1}) of acid sites able to retain pyridine at 150 °C determined with the –OH vibration bands surface area [17]

HF ($\varepsilon = 7.5$ cm μmol^{-1})	HF′ ($\varepsilon = 4.5$ cm μmol^{-1})	LF ($\varepsilon = 5.6$ cm μmol^{-1})	LF′ ($\varepsilon = 4.7$ cm μmol^{-1})
213	99	162	671

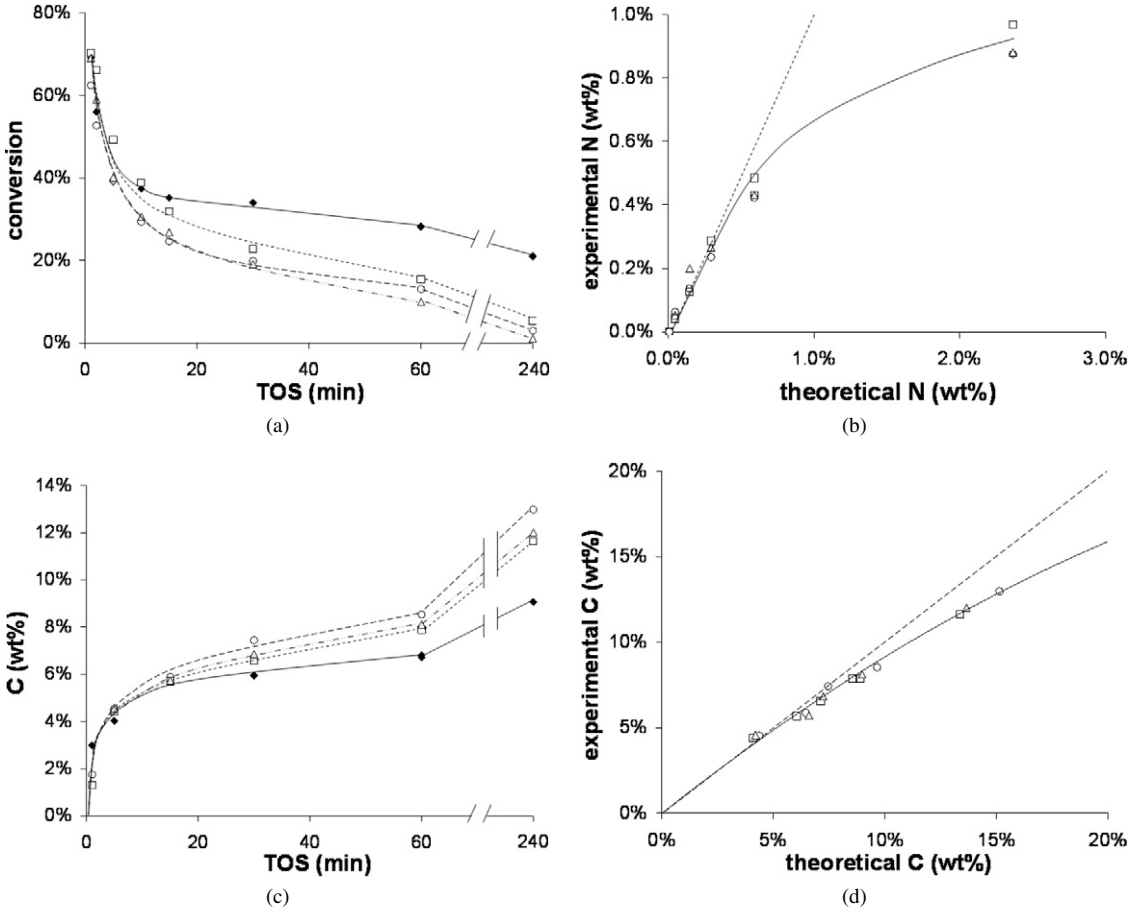

Fig. 2. (a) Methylcyclohexane conversion vs TOS. (b) Experimental nitrogen content vs theoretical nitrogen content. (c) Carbon content in the zeolite vs TOS. (d) Experimental carbon content vs theoretical carbon amount. (◆) Methylcyclohexane alone, (□) methylcyclohexane + 3-methylpyridine, (○) methylcyclohexane + quinoline, and (△) methylcyclohexane + 2,6-dimethylpyridine.

activation. This molecule has the higher proton affinity of the three (963 kJ mol^{-1}). Indeed, this correlation between proton affinity had been reported previously [14,29,30]. Corma et al. [14] explained this effect through an inductive partial deactivation of the neighbor Brønsted sites close to the one interacting with the base.

Besides poisoning the sites responsible by the reaction, nitrogen molecules like 3-methylpyridine, quinoline, and 2,6-dimethylpyridine also can act as coke precursors due their aromatic nature. Fig. 2c shows the evolution of the carbon content during methylcyclohexane transformation; it is shown that basic nitrogen molecules augment the number of carbon atoms in the zeolite, but this does not mean that coke formation rate is enhanced. Instead, the additional amount of carbon can be allocated to the atoms existing in the adsorbed poison molecules.

Fig. 2d clarifies this fact; it represents the actual experimental carbon content in the zeolite versus the amount of carbon calculated as the sum of the carbon amount during the test with methylcyclohexane alone with the amount contained in the poison molecules. The number of nitrogen molecules in the catalyst was determined based on the amount of nitrogen obtained by elemental analysis. This representation proves that poison molecules do not increase coke formation.

3.3. Deactivating molecules characterization

3.3.1. Coke

FT-IR spectra of coked zeolites present several new bands not present in the spectrum of the fresh zeolite, namely in the 2800–3000 cm^{-1} (bands of C–H stretching vibrations) and 1300–1700 cm^{-1} regions (bands of C–H deformation and C–C stretching vibrations) [16,26]. Indeed, for the samples coked with methylcyclohexane alone, bands appear in these two regions of the spectra at 1353, 1413, 1490, 1567, 1600, 1610, 2880, 2934, 2966, 3071, and 3098 cm^{-1} (Figs. 3a and 3b). The integrated surface in the 1300–1700 cm^{-1} region is proportional to the amount of carbon in the zeolite.

3.3.2. Basic nitrogen-containing molecules

For the tests performed with nitrogen, along with the bands noted earlier, others also appear in the same region of the spectra. For the samples containing 3-methylpyridine (Fig. 4a), new bands are easily detectable at 1634, 1560, 1512, 1489, and 1475 cm^{-1}.

For the tests performed with quinoline (Fig. 4b), bands appear at 1302, 1378, 1393, 1413, 1464, 1493, 1515, 1563, 1599, and 1639 cm^{-1}. The bands at 1413 and 1639 cm^{-1} are charac-

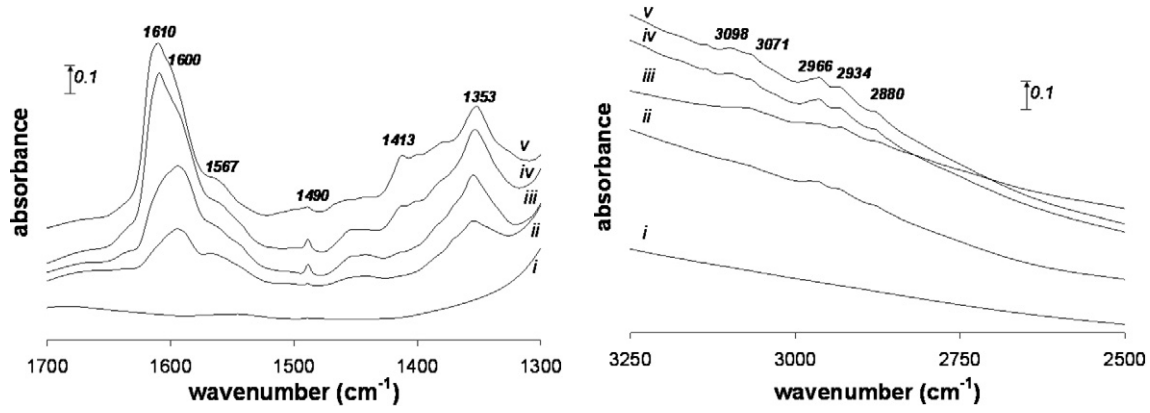

Fig. 3. (a) 1300–1700 cm^{-1} and (b) 2500–3250 cm^{-1} regions of FT-IR spectra of the H-USY(5) zeolite coked with methylcyclohexane alone for (i) 0 min, (ii) 1 min, (iii) 15 min, (iv) 60 min, and (v) 240 min.

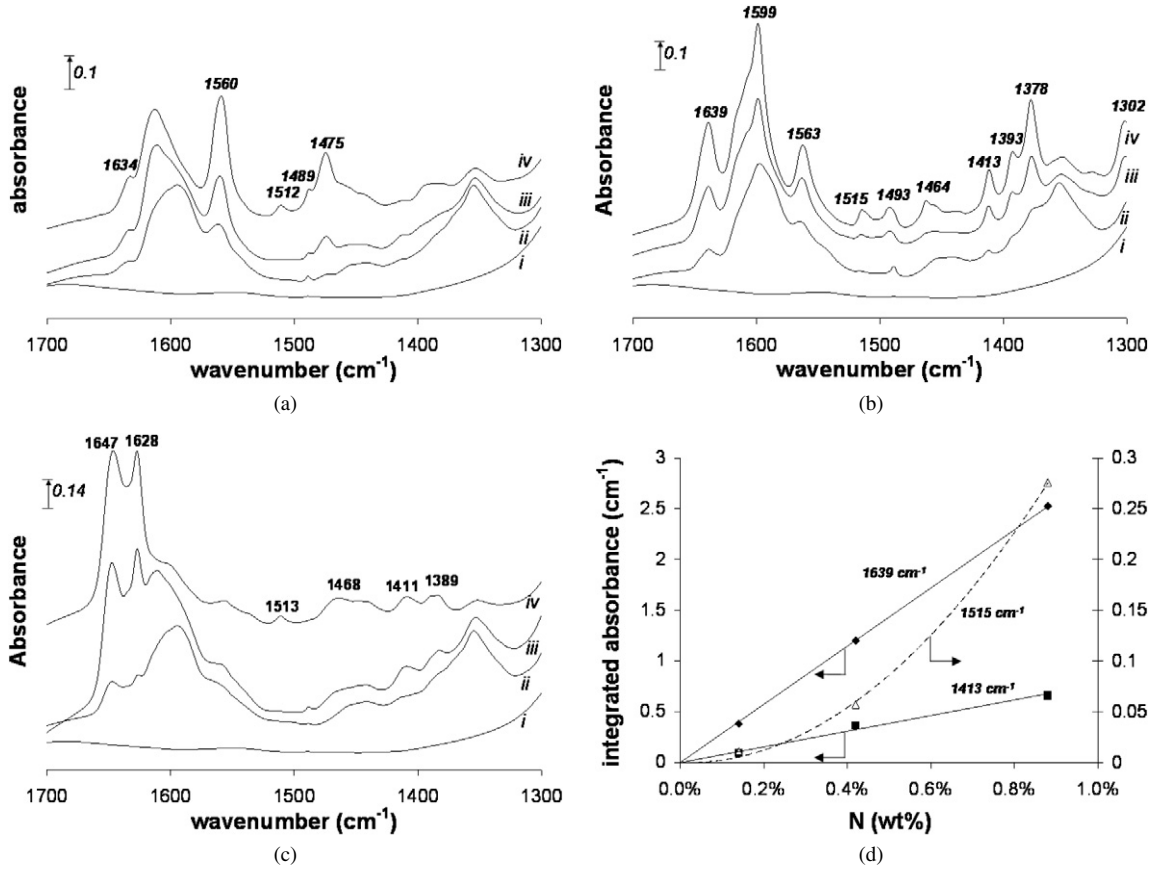

Fig. 4. (a) 1300–1700 cm^{-1} region of FT-IR spectra of the H-USY(5) zeolite coked with (a) methylcyclohexane + 3-methylpyridine, (b) methylcyclohexane + quinoline, and (c) methylcyclohexane + 2,6-dimethylpyridine for (i) 0, (ii) 15, (iii) 60, and (iv) 240 min. (d) Intensity of the (■) 1413, (△) 1515, and (◆) 1639 cm^{-1} bands for the zeolite coked with quinoline vs nitrogen content.

teristic of quinoline molecules adsorbed on Brønsted acid sites [28,31] and correspond to stretching and deformation vibrations of the quinolinium ion. Quinoline molecules coordinated with Lewis acid sites give rise to a band at 1515 cm^{-1}.

Finally, five new bands appear for the zeolites poisoned with 2,6-dimethylpyridine (Fig. 4c). The two intense bands at 1628 and 1647 cm^{-1} agree fairly well with those reported in the literature for protonated species and may be ascribed to vibration modes of 2,6-dimethylpyridinium species [32,33]. The bands characteristic of coordination on Lewis acid sites (1618 and 1580 cm^{-1}) [32,33] are not visible. This means that 2,6-dimethylpyridine, in contrast to quinoline and possibly 3-methylpyridine, does not seem to interact with Lewis acid sites. This can be explained by steric hindrance, which prevents the

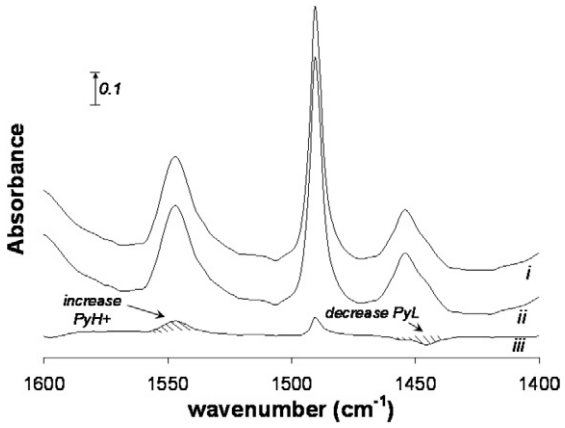

Fig. 5. FT-IR spectra of PyL and PyH^+ bands of the fresh zeolite at 150 °C for a same amount of pyridine (∼300 μmol g^{-1}—before saturation) after contact with the zeolite for (i) 1 min, (ii) $t = 2$ min, and (iii) subtraction spectra (ii − i).

2,6-dimethylpyridine molecules from being adsorbed at Lewis acid centers.

By representing the intensity of the bands characteristic of Lewis and Brønsted acid sites versus the amount of nitrogen in the zeolite, we would expect to obtain some important information about the modes of interaction of the nitrogen molecule with the zeolite. Fig. 4d represents the case for quinoline, for which the attribution of the bands is well known. It is clear that the intensity of the two bands characteristic of the interaction with Brønsted acid sites is more or less proportional to the amount of nitrogen in the zeolite (Fig. 4d). On the other hand, the surface of the 1516 cm^{-1} band is very small for small TOS values but increases exponentially for high TOS, which seems to point out that the interaction with the Lewis acid sites is not preferential. In reality, these results seem to indicate that the coordination with Lewis acid sites happens only after saturation of the protonic sites. However, Lewis sites can still play a role in retaining the nitrogen molecules temporarily before saturation of the protonic sites occurs.

As it was referred earlier, the 2,6-dimethylpyridine molecule does not seem to interact with the Lewis acid sites. This may be one factor explaining its greater poisoning ability. In reality, if a quinoline or a 3-methylpyridine molecule diffuse in the proximity of a Lewis acid sites, then an interaction will always occur, even if it is weaker than toward Brønsted sites. Some of these basic compounds can then desorb and migrate to neighbor Brønsted acid sites. This effect is shown in Fig. 5.

Therefore, even if the majority of the base molecules are adsorbed on the protonic sites, the existence of Lewis sites limits the decrease in activity during the reaction. This would explain why 3-methylpyridine and quinoline deactivate less than 2,6-dimethylpyridine. Even so, for this specific contact time, 3-methylpyridine also deactivates less than quinoline. This can be related to the other relevant property of the nitrogen base: molecular weight. Indeed, quinoline has a ∼15% higher molecular weight than 3-methylpyridine; that has already been reported to be a determining factor [30].

3.4. Deactivated zeolite characterization

3.4.1. Brønsted acidity

3.4.1.1. Al–OH–Si groups vibration bands Fig. 6a shows the decrease in the intensity of the bands corresponding to Al–OH–Si after coking with methylcyclohexane alone. Clearly, a very strong consumption of protonic sites occurs during the first minute of reaction, which is in agreement with the high amount of coke formed for this TOS value. Indeed, this decrease in acid sites provides clear proof of the existence of a very steep deactivation profile between 0 and 1 min, as was proposed earlier. After 15 min, the diminution on the surface of the bands starts to stabilize, congruent with the existence of a plateau in the conversion versus TOS curve.

The better way to compare the deactivation caused by coke and each of the nitrogenated bases is to deconvolute the spectra and quantify the amount of each type of acid sites. The retention of the basic compounds introduces an additional amount of carbon into the zeolite; to sort out this effect, the amount of acid sites is displayed versus the amount of carbon in the catalyst in Figs. 6b–6d.

In terms of the Brønsted acid sites characterized by the HF band (at 3625 cm^{-1}, located in the supercages), the decrease due to coking reaches 55% after only 1 min of reaction (Fig. 6b). Even so, Fig. 6c clearly shows that the hydroxyl groups characterized by the HF′ band (at 3600 cm^{-1}, located in the supercages in interaction with EFAl species) are clearly the most affected by coke (a 71% decrease after 1 min), which can be attributed to their supposedly predominant role in coke formation [34]. In fact, the strong initial deactivation in the H-USY zeolite is due mainly to the poisoning and/or blockage of these acid sites. These Al–OH–Si groups, as discussed previously, are considered quite strong, able to keep the pyridine molecule at very high temperatures. It is relatively well known that over protonic Y zeolites, coke is formed predominately in the supercages [9,26,34,35]; hence the normal rapid decay of the 3625 and 3600 cm^{-1} bands in the first minutes of reaction.

The basic nitrogen-containing molecules seem to intensify the deactivation effect at equal carbon contents. The Brønsted acid sites density decreases more pronouncedly for the tests performed with 3-methylpyridine, quinoline, and 2,6-dimethylpyridine, which means that basic molecules are more toxic than neutral coke molecules

In which regards the hydroxyl groups characterized by the low-frequency bands (LF and LF′), they seem to be less affected both by coke and basic nitrogen compounds (Figs. 6d–6e). They are located in the zeolite sodalite cages, and consequently they normally are not as affected. The most pertinent question in this case is why these acid sites disappear if coke molecules cannot be formed inside the sodalite cages. One should remember that the calculated amount of acid sites corresponds to the acid sites able to interact with the pyridine molecule. Even if the –OH sites present in the sodalite cages are free, this does not mean that they can protonate the pyridine molecule, especially if there are coke molecules in the supercages, which hinder the interaction.

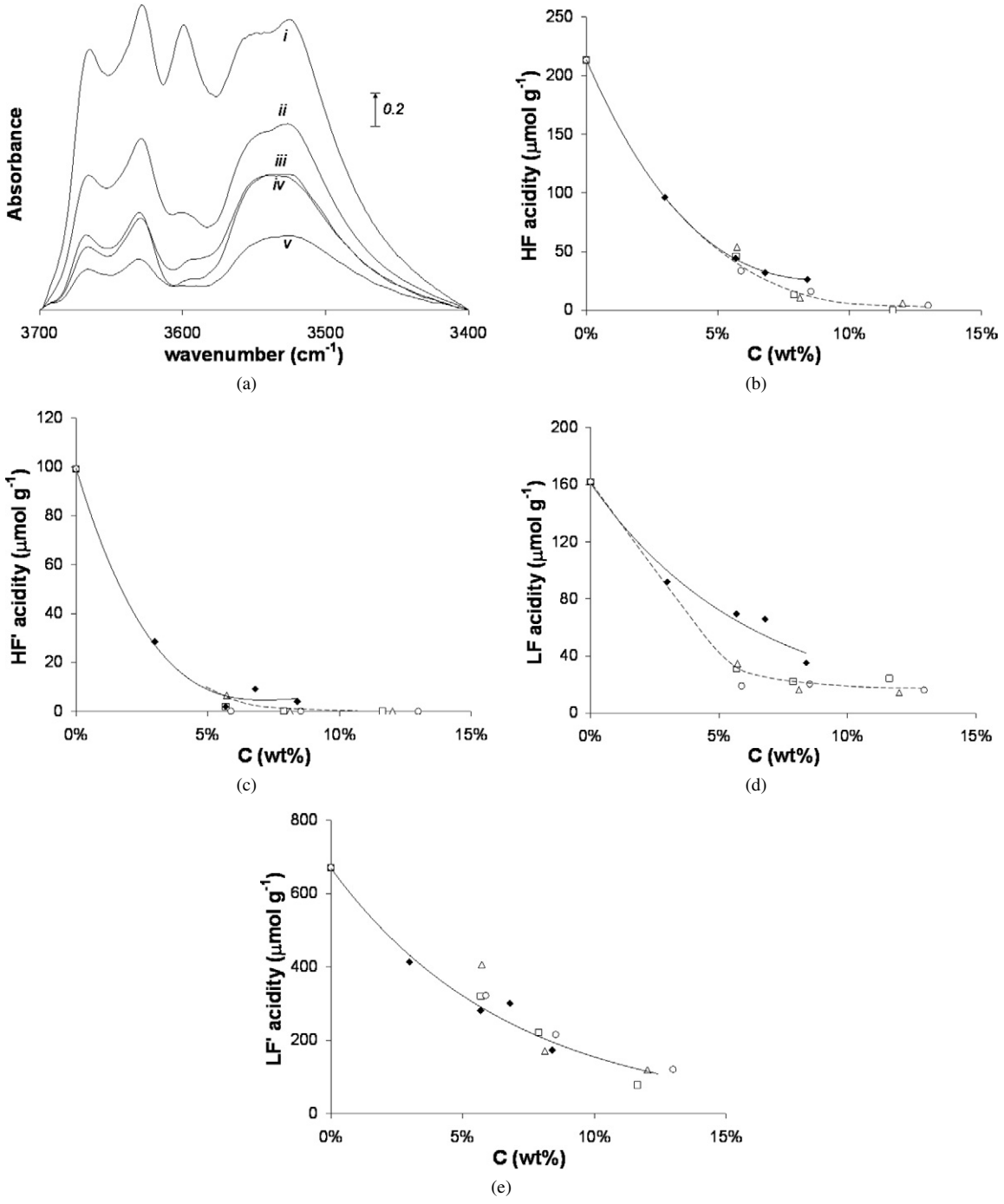

Fig. 6. (a) 3400–3700 cm^{-1} region of FT-IR spectra of the H-USY(5) zeolite coked with methylcyclohexane alone for (i) 0, (ii) 1, (iii) 15, (iv) 60, and (v) 240 min. Amount of (b) HF, (c) HF′, (d) LF, and (e) LF′ Brønsted acid sites vs carbon content. (◆) Methylcyclohexane alone, (□) methylcyclohexane + 3-methylpyridine, (○) methylcyclohexane + quinoline, and (△) methylcyclohexane + 2,6-dimethylpyridine.

3.4.1.2. PyH^+ band In general, the concentration of Brønsted acid sites can be determined from the intensity of the band at 1545 cm^{-1} on pyridine adsorption. In this particular system, this determination is much more complicated because three additional factors must be accounted for (i) exchange between the poisoning molecules (3-methylpyridine, quinoline, and 2,6-dimethylpyridine) and the probe molecule (pyridine); (ii) the basic pyridine molecules can remove the lighter coke molecules from acid sites replacing them; (iii) pyridine molecules can be protonated by the charged coke molecules adsorbed on the acid sites.

Fig. 7a represents the displacement of coke formed without basic nitrogen on pyridine adsorption. Clearly, there are numerous coke molecules, which desorb to provide a space for the probe molecule (pyridine). This means that the amount of PyH^+ will be higher than the value of free and accessible Al–OH–Si groups in the zeolite. The referred phenomenon is more intense for samples deactivated for short TOS. In contrast, coke

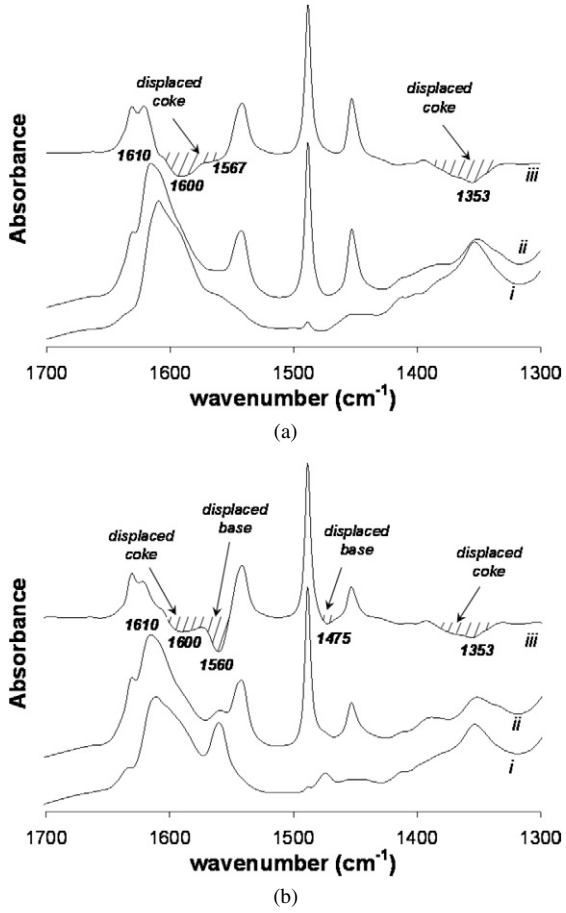

Fig. 7. (a) Decrease in the bands characteristic of coke upon pyridine adsorption at 150 °C for the sample coked with methylcyclohexane alone for 60 min. (b) Decrease in the bands characteristic of coke and nitrogen bases upon pyridine adsorption at 150 °C for the sample coked with methylcyclohexane + 3-methylpyridine for 60 min: (i) IR spectrum without pyridine, (ii) IR spectrum after pyridine adsorption, and (iii) difference spectrum.

formed after 240 min (9.07 wt% C) is heavier and more difficult to desorb. The error is even greater for the measurements performed in the samples containing basic nitrogen. In fact, pyridine, due to its much higher partial pressure, will cause the other base to desorb and take its place; the effect will be even more pronounced if the basicity of the tested nitrogen base is inferior to the one of pyridine. Fig. 7b shows the displacement of 3-methylpyridine molecules during pyridine adsorption; more than half of the 3-methylpyridine molecules desorb.

3.4.2. Lewis acidity

The evolution of the amount of Lewis acid sites during deactivation is also relevant; however, the number of Lewis sites does not decrease visibly during deactivation. In fact, for some TOS values, the Lewis acid site density is even greater than for the fresh zeolite. Maybe the actual coke molecules can act as Lewis acid sites. Indeed, positively charged species are known to be rather strong Lewis sites. Despite this detail, the results seem to indicate that the Lewis acid sites are affected only slightly by coke formation and nitrogen poisoning. In fact, differences are visible only at 5–6 wt% of retained carbon.

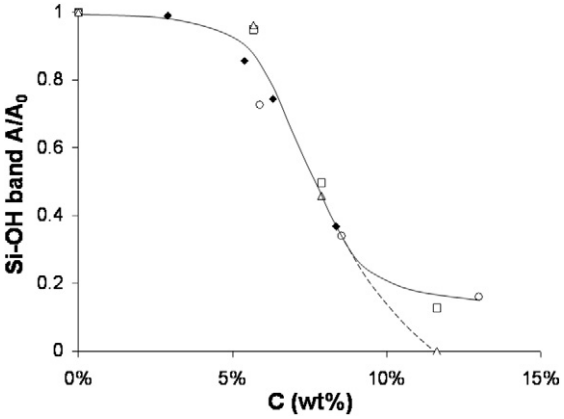

Fig. 8. Global surface of the Si–OH bands in the 3800–3700 cm^{-1} region vs carbon content: (◆) methylcyclohexane alone, (□) methylcyclohexane + 3-methylpyridine, (○) methylcyclohexane + quinoline, and (△) methylcyclohexane + 2,6-dimethylpyridine.

3.4.3. Mesopores and external surface (Si–OH groups)

The 3800–3700 cm^{-1} region of the spectra exhibits the bands characteristic of silanol groups. The Si–OH groups occur in defects and on the external surface of crystallites. The decreased amount of silanol groups is normally due to the formation of bulkier coke molecules that grow out to the zeolite crystallites external surface. For this reason, this measurement can be used as an indicator of the amount of coke deposed in the external surface. Fig. 8 shows that up to 5–6 wt% of coke, there is almost no decrease in the amount of silanols, indicative of the low affinity of the poison molecules toward silanols compared with Al–OH–Si groups. However, from this point on, the amount of external silanols decreases significantly with carbon content, which must correspond to formation of coke on the crystallite external surface.

The presence of basic nitrogen does not seem to have any particular effect on the amount of silanol groups, except for the 2,6-dimethylpyridine molecule, which eliminates all of the Si–OH groups after 4 h of reaction. This must be linked to its larger kinetic diameter (6.7 Å); when the zeolite microporous structure begins to saturate, this molecule must experience some difficulty entering the zeolite micropores, and consequently must adsorb preferentially onto the acid silanols.

3.5. Acidity–activity correlations

It is widely accepted that the activity of a protonic zeolite for a given hydrocarbon transformation should increase as its Brønsted acidity increases. The easiest way to obtain zeolites with different acid site densities is to submit several samples of the same parent zeolite to different dealumination treatments to extract the FAl (framework Al) responsible for the Brønsted acidity. The loss in acid sites will depend on the severity of the treatment. This treatment can cause other changes in the microporous structure and acid strength as well. For this reason, among others, some investigations have included the acid strength in the equation, with promising results [36–39].

The study of deactivation also allows the study of the relation between the catalyst activity and acidity. In this case, no

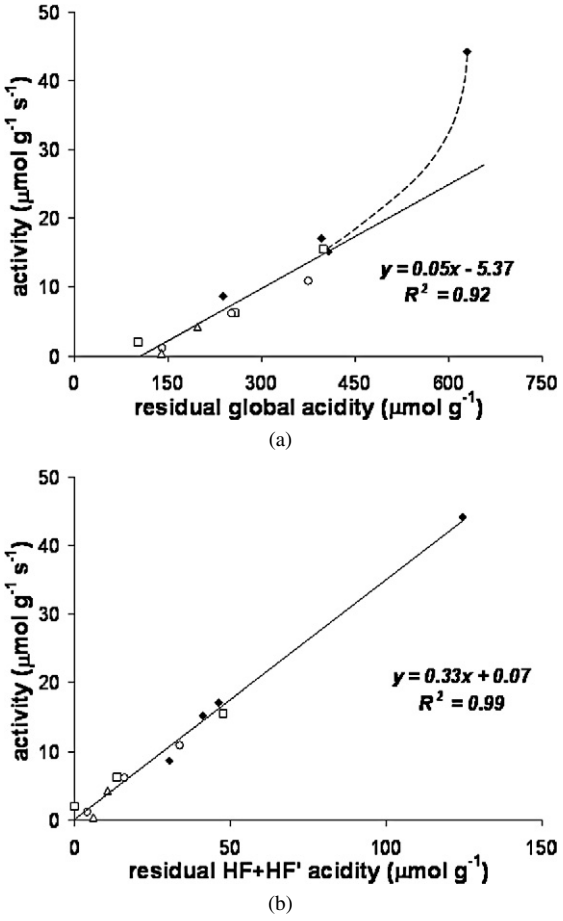

Fig. 9. (a) Activity vs global Brønsted acidity. (b) Activity vs high frequency Brønsted acidity. (◆) Methylcyclohexane alone, (□) methylcyclohexane + 3-methylpyridine, (○) methylcyclohexane + quinoline, and (△) methylcyclohexane + 2,6-dimethylpyridine.

treatment was done, and, consequently, the acid sites properties remained unchanged. In addition, although in other studies, the initial activity (which already includes some deactivation) is compared with the fresh zeolite acidity, here this aspect was taken into consideration. Indeed, the initial activity is compared with the acidity after 1 min of reaction, for which almost half of the fresh H-USY acidity is gone. The activity was determined with the following equation, assuming a plug-flow reactor and an overall order of 1 in terms of the reactant:

$$a\ (\mu\text{mol g}^{-1}\,\text{min}^{-1}) = \frac{\ln[(1-X)^{-1}]\text{WHSV}}{\text{MW}}, \qquad (1)$$

where X is the conversion, a is the zeolite activity, WHSV is the weight hourly space velocity, and MW is the reactant molecular weight. Fig. 9a represents the activity versus the global acidity (Brønsted sites able to adsorb pyridine at 150 °C based on the –OH vibration bands) of the H-USY zeolite. Two facts are evident: (i) the initial decrease in activity (1 min → 15 min) is very high compared with the decrease in acidity, and (ii) the activity reaches zero when a reasonable amount of free and accessible Brønsted acid sites remains (107 μmol g^{-1}, obtained by extrapolation). Clearly, some of the acid sites do not seem to participate in the transformation of methylcyclohexane (isomerization, cracking, or hydrogen transfer). Interestingly, these inactive acid sites corresponded exclusively to low-frequency acid sites; all of the high-frequency acid sites (HF + HF′) were poisoned and/or blocked for the tests with the nitrogen-containing bases after 240 min of reaction.

Comparing the activity exhibited by the zeolite with the high-frequency acidity (supercages) alone demonstrates that the correlation is significantly improved (Fig. 9b). First, the correlation is always linear for the analyzed acidity intervals, and, second, the activity is very close to zero when the high-frequency acidity disappears. Consequently, it can be safely concluded that the high-frequency sites are the main active sites of the methylcyclohexane reaction. Another argument supporting this hypothesis is the behavior shown in Fig. 9a. Indeed, the strong decrease in activity observed in the first minutes of reaction, which is not accompanied by a strong decrease in the global acidity, should be caused by the rapid poisoning of the high-frequency sites in these initial minutes.

These observations seem to agree with the fact that the methylcyclohexane molecule does not access the sodalite cages where the low-frequency sites are located. Even if the protons have some mobility, the acid sites located in the sodalite cages should exhibit low activity compared with the Al–OH–Si groups in the supercages.

The turnover frequency (TOF) of a zeolite expresses the activity of each one of its active sites. More precisely, it quantifies the average number of reactant molecules transformed in each active site per unit of time. The TOF of an acid catalyst like the H-USY zeolite can be calculated by dividing its activity by its acidity before the reaction. However, the measured initial activity can include a strong initial deactivation; thus, only one point of the activity versus acidity curve is used in the calculations, which introduces a great deal of uncertainty into the TOF value. A more accurate formula is

$$\text{TOF}\ (\text{min}^{-1}) = \frac{da\ (\mu\text{mol g}^{-1}\,\text{min}^{-1})}{d[\text{HZ}]\ (\mu\text{mol g}^{-1})}, \qquad (2)$$

where [HZ] is the Brønsted sites density and $da/d[\text{HZ}]$ is the slope of the curve between the activity and the Brønsted acidity of the studied zeolite during deactivation. This formula corresponds to the IUPAC definition of TOF. The calculated value is 0.05 molecules s^{-1} when considering the overall acidity (Fig. 9a) and 0.33 molecules s^{-1} when considering only the high-frequency acidity (Fig. 9b). For the reasons noted earlier, the second value is much closer of the actual TOF of the active sites in the H-USY zeolite. The first TOF value includes numerous sites that are not active and for this reason is inadequate. Conversely, when considering the acidity of the fresh zeolite corresponding only to the high-frequency bands (312 μmol g^{-1}), the value thus obtained is 0.14 molecules s^{-1}, which is less than half the actual value calculated with the slope of the activity versus acidity curve.

4. Conclusions

The results presented in this paper elucidate various aspects of the deactivation during catalytic cracking reactions.

Although the fact that coke formation and nitrogen poisoning had already been studied by other research groups, this work contributes with several new facts that add to the knowledge in this area. In addition, this is the first work that accounts for the two phenomena simultaneously; indeed, it was shown that the two cannot be dissociated.

Coke formation induces a strong decrease in zeolite activity, especially in the first minutes of the reaction. The acid sites in the supercages are the first to be affected by coke deposition. The adsorption of basic nitrogen compounds also causes a reduction in the activity of acid USY zeolites. The fact is clearly due to the almost irreversible interaction of these basic molecules with the Brønsted acid sites, which catalyze all of the studied reactions. In fact, nitrogen poisons seem to adsorb preferentially on these sites, even if coordination on the zeolite Lewis acid sites is also feasible. As before, the sites located in the supercages are the first to be poisoned, probably because the others are not accessible. Basic nitrogen molecules seem more toxic than neutral coke molecules.

Quantification of the PyH^+ band on pyridine adsorption is an inaccurate method for monitoring the decrease in the amount of Brønsted acid sites during the deactivation of catalytic cracking catalysts. In fact, this probe desorbs the poisoning molecules (coke and nitrogen molecules) already adsorbed on the acid sites, resulting in overestimation of the number of accessible acid sites. For this reason, only the decrease of the bands corresponding to the Al–OH–Si groups can be used to determine the actual amount of possibly active Brønsted acid sites.

The poisoning effect varies with the physicochemical properties of the poisoning base. The 2,6-dimethylpyridine molecule appears to have greater poisoning ability than the other two bases tested (3-dimethylpyridine and quinoline). One explanation can be proposed based on our findings: 2,6-dimethylpyridine molecules interact exclusively with the Brønsted acid sites, in contrast to the other two bases, which also are adsorbed on Lewis acid sites. This is due to steric hindrance, which prevents adsorption of the 2,6-dimethylpyridine molecules at Lewis acid sites. Consequently, the deactivation is more pronounced for the first base. Alternative explanations include an inductive poisoning effect of the neighbor sites. The extent of this effect will increase with the protonic affinity of the poisoning base, and because 2,6-dimethylpyridine has the highest value, it should produce the highest deactivation.

Acidity–activity correlations show that the Brønsted acid sites characterized by the –OH high-frequency bands are the main cause of the methylcyclohexane transformation. An average TOF value was determined with the slope of the activity versus high-frequency acidity curve: 0.33 s^{-1}. This value is more than twice the TOF calculated with the initial activity and the fresh zeolite Brønsted acidity characterized by the same high-frequency bands.

Acknowledgments

This work was funded by the Fundação para a Ciência e Tecnologia (FCT) (project POCI/EQU/58550/2004). The first author also was supported by a doctoral grant from the FCT (SFRH/BD/13411/2003).

References

[1] J. Thomas, F. Degnan, Top. Catal. 13 (2000) 349.
[2] N. Katada, Y. Kageyama, K. Takahara, T. Kanai, H.A. Begum, M. Niwa, J. Mol. Catal. A Chem. 211 (2004) 119.
[3] B.H. Wouters, T. Chen, P.J. Grobet, J. Phys. Chem. B 105 (2001) 1135.
[4] D.L. Bhering, A. Ramirez-Solis, C.J.A. Mota, J. Phys. Chem. B 107 (2003) 4342.
[5] B.A. Williams, S.M. Babitz, J.T. Miller, R.Q. Snurr, H.H. Kung, Appl. Catal. A Gen. 177 (1999) 161.
[6] F. Lemos, F.R. Ribeiro, M. Kern, G. Giannetto, M. Guisnet, Appl. Catal. 29 (1987) 43.
[7] F. Lemos, F.R. Ribeiro, M. Kern, G. Giannetto, M. Guisnet, Appl. Catal. 39 (1988) 227.
[8] F. Maugé, P. Gallezot, J.C. Courcelle, P. Engelhard, J. Grosmangin, Zeolites 6 (1986) 261.
[9] M. Guisnet, P. Magnoux, Appl. Catal. A Gen. 212 (2001) 83.
[10] M. Guisnet, P. Magnoux, App. Catal. 54 (1989) 1.
[11] G.D. Hobson, Modern Petroleum Technology—Part I, Wiley, New York, 1992.
[12] A. Corma, F.A. Mocholí, Appl. Catal. A Gen. 84 (1992) 31.
[13] J. Scherzer, D.P. Mcarthur, Ind. Eng. Chem. Res. 27 (1988) 1571.
[14] A. Corma, V. Fornes, J.B. Monton, A.V. Orchilles, Ind. Eng. Chem. Res. 26 (1987) 882.
[15] G. Caeiro, P. Magnoux, J.M. Lopes, F.R. Ribeiro, Appl. Catal. A Gen. 292 (2005) 189.
[16] J. Ryczkowski, Catal. Today 68 (2001) 263.
[17] S. Khabtou, T. Chevreau, J.C. Lavalley, Micropor. Mater. 3 (1994) 133.
[18] N. Echoufi, P. Gélin, Catal. Lett. 40 (1996) 249.
[19] M.A. Makarova, K. Karim, J. Dwyer, Micropor. Mater. 4 (1995) 243.
[20] C.A. Emeis, J. Catal. 141 (1993) 347.
[21] F. Thibault-Starzyk, B. Gil, S. Aiello, T. Chevreau, J.-P. Gilson, Micropor. Mesopor. Mater. 67 (2004) 107.
[22] M. Guisnet, P. Ayrault, J. Datka, Pol. J. Chem. 71 (1997) 1455.
[23] M.A. Makarova, J. Dwyer, J. Phys. Chem. 97 (1993) 6337.
[24] W. Zhang, E.C. Burckle, P.G. Smirniotis, Micropor. Mesopor. Mater. 33 (1999) 173.
[25] J. Datka, B. Gil, P. Baran, J. Mol. Struct. 645 (2003) 45.
[26] H.S. Cerqueira, P. Ayrault, J. Datka, M. Guisnet, Micropor. Mesopor. Mater. 38 (2000) 197.
[27] A. Zecchina, S. Bordiga, G. Spoto, D. Scarano, G. Petrini, G. Leofanti, M. Padovan, J. Chem. Soc. Faraday Trans. 88 (1992) 2959.
[28] A. Corma, V. Fornés, F. Rey, Zeolites 13 (1993) 56.
[29] C.-M. Fu, A.M. Schaffer, Ind. Eng. Chem. Prod. Res. Develop. 24 (1985) 68.
[30] T.C. Ho, A.R. Katritzky, S.J. Cato, Ind. Eng. Chem. Res. 31 (1992) 1589.
[31] T.J. Dines, L.D. MacGregor, C.H. Rochester, Langmuir 18 (2002) 2300.
[32] T. Onfroy, G. Clet, M. Houalla, Micropor. Mesopor. Mater. 82 (2005) 99.
[33] C. Morterra, G. Cerrato, G. Meligrana, Langmuir 17 (2001) 7053.
[34] M. Guisnet, P. Magnoux, in: B. Delmon, et al. (Eds.), Catalyst Deactivation, in: Studies in Surface Science and Catalysis Series, vol. 88, Elsevier, Amsterdam, 1994.
[35] M. Guisnet, P. Magnoux, D. Martin, in: C.H. Bartholomew, et al. (Eds.), Catalyst Deactivation, in: Studies in Surface Science and Catalysis Series, vol. 111, Elsevier, Amsterdam, 1997.
[36] C. Costa, J.M. Lopes, F. Lemos, F. Ramôa Ribeiro, Catal. Lett. 44 (1997) 255.
[37] C. Costa, J.M. Lopes, F. Lemos, F. Ramôa Ribeiro, J. Mol. Catal. A Chem. 144 (1999) 233.
[38] C. Costa, I.P. Dzikh, J.M. Lopes, F. Lemos, F. Ramôa Ribeiro, J. Mol. Catal. A Chem. 154 (2000) 193.
[39] P. Borges, R.R. Pinto, M.A.N.D.A. Lemos, F. Lemos, J.C. Védrine, E.G. Derouane, F.R. Ribeiro, J. Mol. Catal. A Chem. 229 (2005) 127.